Chemical zonation in the Upper Bandelier Tuff: Evidence from the chemistry of distal outcrops, Puye quadrangle

David P. Dethier, Stephanie K. Kampe, David A. Sawyer, and James R. Budahn
2007, pp. 333-343. https://doi.org/10.56577/FFC-58.333

in:

Geology of the Jemez Region II, Kues, Barry S., Kelley, Shari A., Lueth, Virgil W.; [eds.], New Mexico Geological Society 58 th Annual Fall Field Conference Guidebook, 499 p. https://doi.org/10.56577/FFC-58

This page is intentionally left blank to maintain order of facing pages.

CHEMICAL ZONATION IN THE UPPER BANDELIER TUFF: EVIDENCE FROM THE CHEMISTRY OF DISTAL OUTCROPS, PUYE QUADRANGLE

DAVID P. DETHIER,[1] STEPHANIE K. KAMPF,[2] DAVID A. SAWYER [3], AND JAMES R. BUDAHN [3]
[1]Department of Geosciences, Williams College, Williamstown, Massachusetts 01267, ddethier@williams.edu
[2]Department of Forest, Rangeland & Watershed Stewardship, Colorado State University, Fort Collins, CO 80523-1472
[3]U. S. Geological Survey, P.O. Box 25046, Denver, CO 80225

Abstract — Upper Bandelier Tuff (UBT) exposed beneath finger mesas on the northeastern Pajarito Plateau, New Mexico, includes some of the most distal outcrops of the compound cooling unit erupted from the Valles caldera at about 1.22 Ma. We report major and trace-element analyses for 35 samples of UBT from 8 sites in the Puye quadrangle as well as for 16 samples collected previously from 2 locations in the Los Alamos National Laboratory (LANL) area. Concentrations of silica, sodium, potassium and some other major oxides in UBT units 1 to 4 reflect the evolution from high-silica to low-silica rhyolite during the eruption, but changes are small and grouped data suggest that only TiO_2 varies systematically in the 10 stratigraphic sections. Multiple measurements from 10 sites indicate that concentrations of oxides and trace elements such as Eu, Sr and Zr in units 1 to 3 show little lateral or vertical variation across the area. In vertical sections through the tuff, trace elements such as Rb, Cs, U and Zn display a consistent pattern of zonation. Apparent concentration changes and patterns of relatively low versus high variance in the trace element content within UBT unit 1 may result from local mineralogic control or elemental redistribution during vapor-phase alteration. Trace element chemistry from tuff at Mesas 19 and 25 is anomalous and suggests that field identification of the units may be incorrect or that other processes may affect trace-element zonation in the thinnest distal tuffs.

INTRODUCTION

Upper Bandelier Tuff (UBT) exposed beneath finger mesas on the eastern Pajarito Plateau, New Mexico, includes some of the most distal outcrops of the compound cooling unit erupted from the Valles caldera at about 1.22 Ma (Fig. 1). Mineralogic, physical and chemical characteristics of stratigraphic units of the UBT, first described by Smith and Bailey (1966), have been analyzed in detail for studies ranging from volcanology to vadose-zone hydrology and environmental restoration. Stratigraphic subdivision of the UBT (Broxton and Reneau, 1995) into a basal fall unit (Tsankawi Pumice Bed) and four units of the Tshirege Tuff reflects the distribution of surge beds, degree of welding, color, a prominent boundary between glassy and devitrified tuff, and other characteristics that can be readily mapped (Fig. 2). Accurate identification of stratigraphic intervals is of critical importance for correlations used in studies of paleoseismicity, waste migration and environmental restoration, particularly for subsurface samples. UBT chemistry supports the stratigraphic assignments of Broxton and Reneau (1995), ranging from high-silica rhyolite near the base (unit 1) to low-silica rhyolite in unit 4 near the top of the section. Phenocryst mineralogy changes from predominantly sanidine and quartz in unit 1 to anorthoclase and pyroxene in units 3 and 4. The major-element chemistry of whole-rock samples, however, generally does not allow unambiguous assignment of tuff samples to stratigraphic units. Trace elements in tuffs are more sensitive to gradients in magma chambers and partitioning between melt and vapor (Wilson and Hildreth, 1997), as well as to mobilization during cooling of pyroclastic flows and their subsequent diagenesis (Stimac et al., 1996).

Detailed studies of tuff chemistry at several sites at Los Alamos National Laboratory (LANL) suggests that UBT units, particularly 3 and 4, contain distinctive concentrations of TiO_2

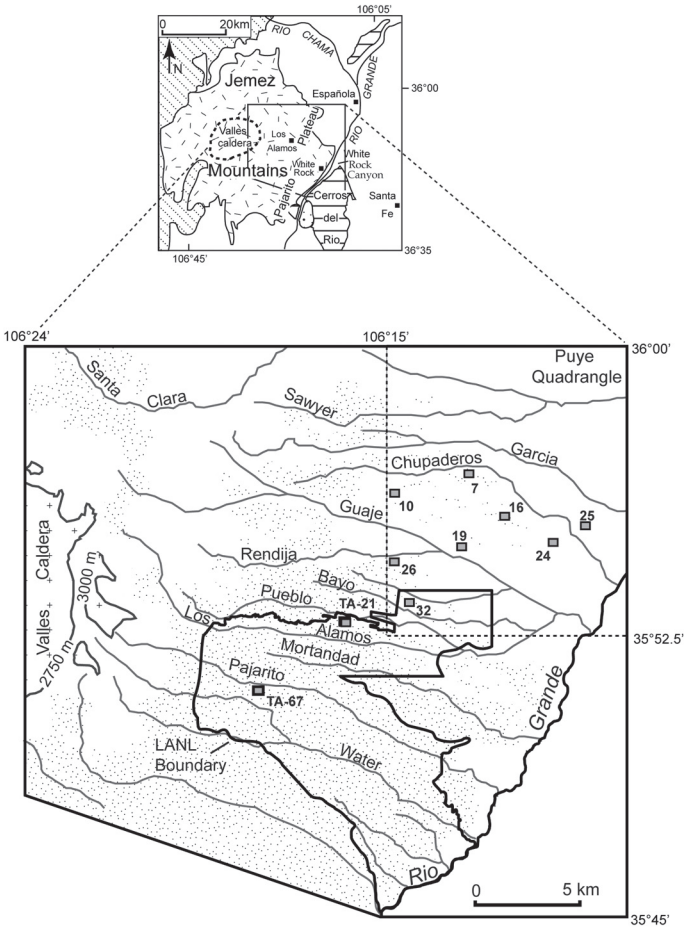

FIGURE 1. Map showing location of the Valles caldera, the Pajarito Plateau, the western Puye quadrangle, and Los Alamos National Laboratory (LANL). Stippled areas are Bandelier Tuff; numbered locations are mesas sampled for tuff chemistry (dashed rectangle in upper right corner shows the area of Fig. 3). Inset shows the Jemez Mountains and nearby features noted in the text.

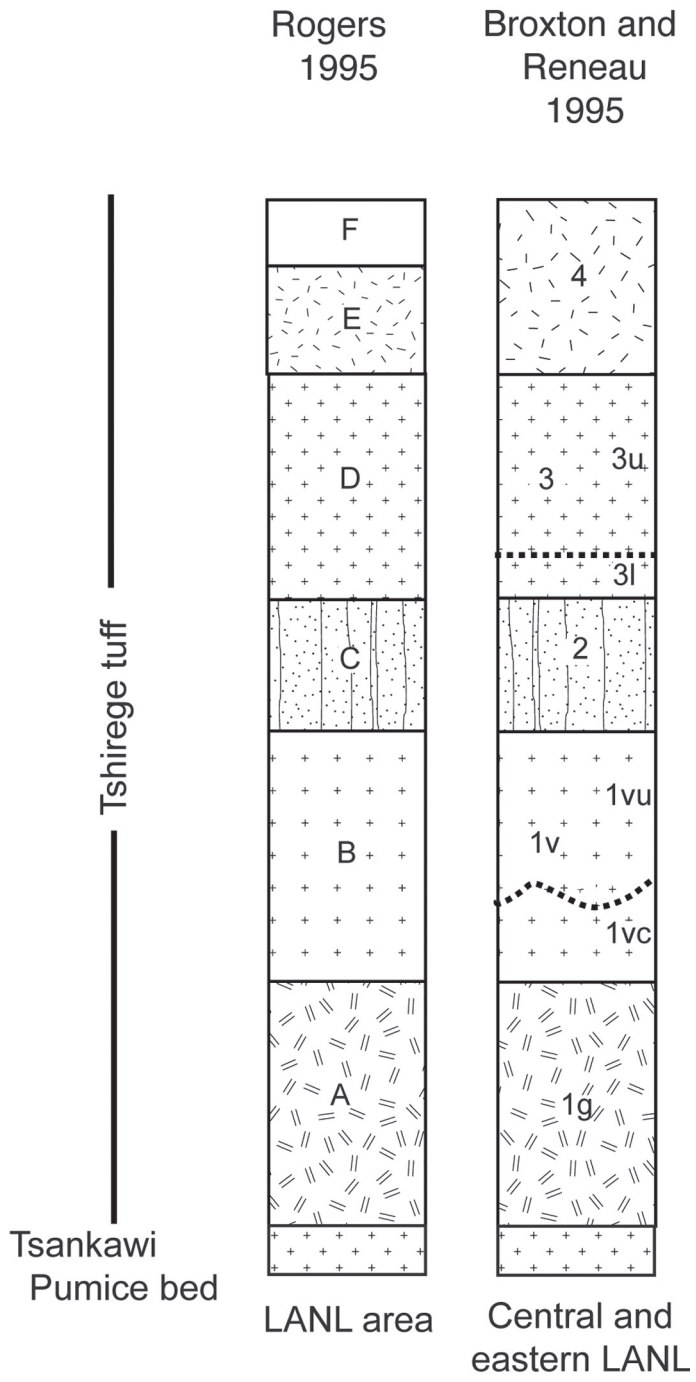

FIGURE 2. Correlation of unit divisions of the Tshirege Member, upper Bandelier Tuff (after Broxton and Reneau, 1995; Rogers, 1995) and Tsankawi Pumice Bed. We informally subdivided unit 3 into lower and upper intervals for our sampling.

and of minor elements such as U, Th, Nb and Rb (Smith and Bailey, 1966; Broxton et al., 1995a; Rogers, 1995; Stimac et al., 2002). Chemical analyses of UBT units (Broxton et al., 1995b) suggest that the range of concentration within tuff units is less than variation between units. However, there has not been extensive analysis of gradients in trace-element chemistry among sites, nor of chemical changes from the thick, relatively proximal UBT sections to the thinner, more distal outcrops typical of the eastern Pajarito Plateau. In this study we compare the chemistry of UBT at LANL sites to that measured on mesas in the Puye quadrangle, some 5 to 15 km more distant from the caldera rim. We emphasize INAA (neutron activation analysis) results from Puye samples and from samples collected in the LANL area.

METHODS

Field studies

Our field studies of the UBT in the Puye quadrangle involved mapping the distribution of the tuff, analyzing stratigraphic sections and sampling of UBT units on selected mesas (Figs. 1, 3). We identified contacts between different units using criteria developed on the main part of the Pajarito Plateau (Broxton and Reneau, 1995). The vapor-phase notch (vpn), the contact between the glassy lower portion and upper devitrified part of unit 1, persists throughout the study area, and the surge units and change in welding that typify the transition between units 1 and 2 are present in many stratigraphic sections. However, we noted surge units and distinctive gradients in welding at the contact between units 2 and 3 at only a few locations. Unit 4 is absent in the Puye quadrangle and extends only a short distance into the western LANL area. We collected samples of tuff from UBT units at 8 mesas (Fig. 1), channel-sampling surface exposures over vertical distances of 1 to 3 m. In sampling we avoided pumice and lithic concentrations and fracture surfaces coated with secondary minerals. Our sampling and bulk chemical analyses are thus representative of a particular zone within a unit, but not necessarily of the entire unit.

Field measurement and sampling procedures in the LANL area involved detailed characterization of the UBT at DP Mesa (TA-21), Pajarito Mesa (TA-67), and adjacent areas as part of the environmental restoration program (Broxton and Eller, 1995; Reneau and Raymond, 1995). Bulk samples of UBT were collected at ~5 to 10 m intervals at several stratigraphic sections and characterized for a wide variety of physical, mineralogic and chemical parameters. The UBT is ~90 m thick at TA-21 and TA-67, but unit 1g is not exposed at TA-21.

Analytical techniques

Bulk samples of UBT were prepared and analyzed by X-ray fluorescence (XRF) techniques at the U. S. Geological Survey (USGS) and at LANL (Broxton et al., 1995b), and by neutron activation (INAA) at the USGS. LANL XRF techniques involved measuring major and selected trace elements using an automated Rigaku wavelength-dispersive spectrometer on crushed, homogenized samples fused with a lithium borate flux (Broxton et al., 1995b). At the USGS the oxide abundances of ten major and minor rock-forming elements (SiO_2, TiO_2, Al_2O_3, total Fe reported as Fe_2O_3, MgO, CaO, Na_2O, K_2O, P_2O_5, MnO) of the rock samples were determined by wave-length-dispersive x-ray fluorescence (WD-XRF). To obtain loss on ignition (LOI), a 0.8 g portion of sample was ignited at 925° C for 45 minutes. The sample was then fused with lithium borate flux to create a

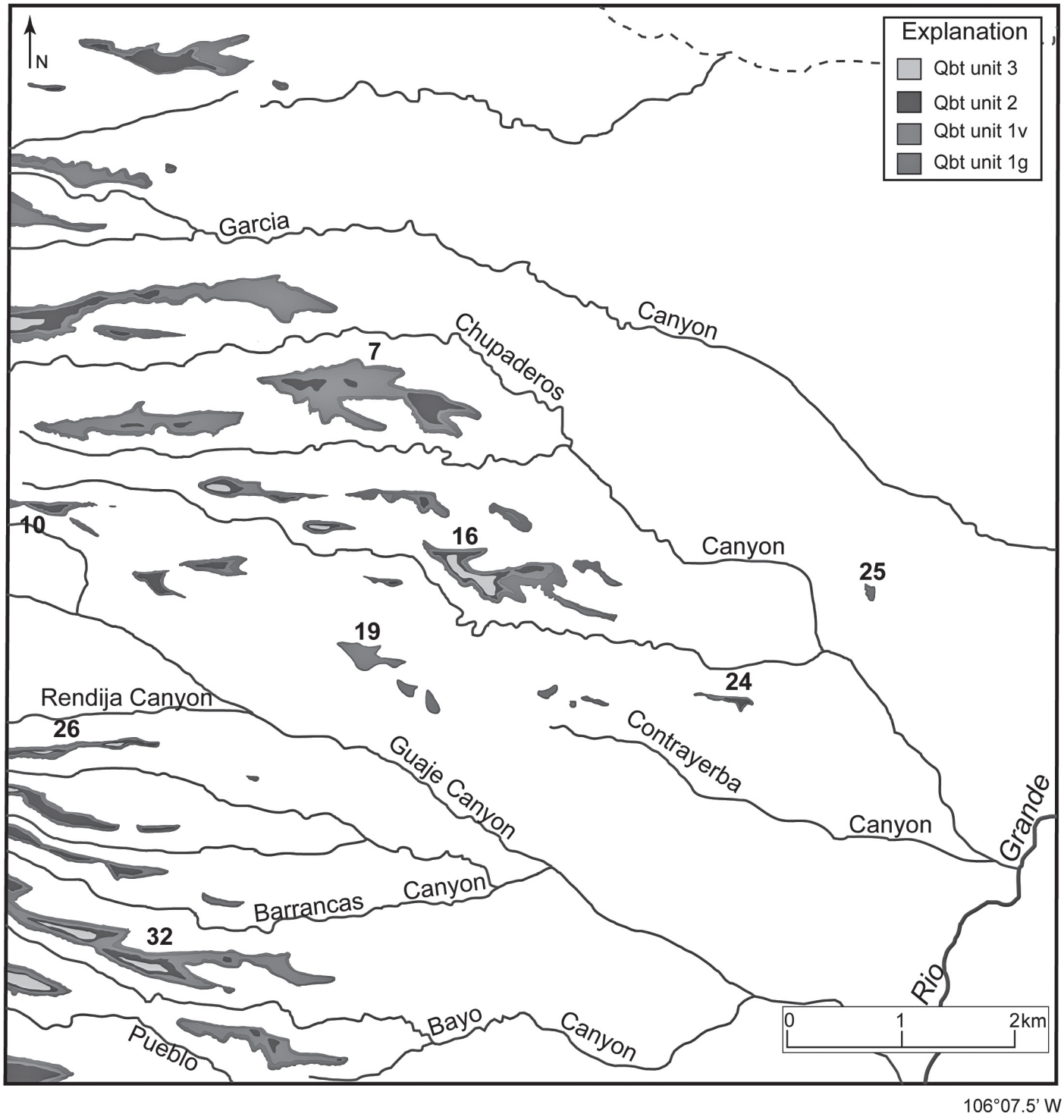

FIGURE 3. Map showing the distribution of Tshirege units exposed on mesas in the Puye quadrangle. Numbered mesas were sampled for chemical analysis.

homogeneous pellet for analysis. The precision of the major- and minor-elemental determinations is typically better than 1%, based on replicate analysis of prepared standards, whereas accuracy is better than 2% based on the results of USGS standard reference materials. A full description of the WD-XRF technique was given by Taggart and Siems (2002).

The abundances of 33 major, minor, and trace elements, including 11 rare-earth elements (REE), were determined on the bulk tuff samples by instrumental neutron activation analysis (INAA). Samples of ~ 1 gram were irradiated in the USGS-TRIGA reactor at a flux of 2.5×10^{12} neutrons/cm^2/sec for eight hours. Three sequential counts at 7 days, 14 days, and 65 days after the irradia-

tion were made on both coaxial and planar germanium detectors. A summary of the INAA procedure used at the USGS was given by Budahn and Wandless (2002). Precision and accuracy for most of the elements determined range from 1 to 5 %, including La, Yb, Hf, Ta, Rb, Th, and U. Only five elements have precision errors of greater than 10% (Ho, Tm, W, Sb, Au) based on counting statistic errors. Accuracy is based on replicate analysis of USGS standard reference materials, including BHVO-1. Sarna-Wojcicki and Davis (1991) reported that between 15 and 20 elements have proved useful in characterizing and distinguishing many silicic tephra samples: Sc, Mn, Fe, Zn, Rb, Cs, Ba, La, Ce, Nd, Sm, Eu, Tb, Dy, Yb, Lu, Hf, Ta, Th, and U.

RESULTS

We report major and trace-element analyses for 35 samples of UBT from 8 sites in the Puye quadrangle, as well as for 16 samples previously collected in the LANL area (Figs. 1, 3; Appendix A). Data from TA-67 do not include INAA analyses and include values for several elements, notably Nb, that were not analyzed in some other samples. Tungsten concentrations in samples from TA-21 were contaminated during sample preparation and are not included in the graphs plotted below. Field stratigraphic relations are reasonably consistent with those portrayed in Figure 2, but units 2 and 3 are thin in most distal exposures of UBT in the Puye quadrangle. Units 1g and 1v are present at each section, but unit 2 is relatively thin in most of the northern area. Areas of unit 3 cap several mesas in the southwest and central portions of the Puye quadrangle. Analyses of unit 4 plotted below are from the western LANL area.

Major-element chemistry

Concentrations of silica, sodium, potassium and other major oxides in units 1 to 4 reflect the evolution from high-silica to low-silica rhyolite over the course of the UBT eruption, but changes are small and grouped data (Appendix A; Fig. 4) suggest that there are no systematic variations among the 10 stratigraphic sections. Unit 4 samples have SiO_2 values between 72.5 and 74.5%, as does one sample of unit 1 g; most samples in units 1 to 3 fall between 75.5 and 77.5% SiO_2. Calcium and sodium (Fig. 4) and potassium, and Fe O concentrations overlap at the 1σ level in units 1g through 3. $^{2}Fe^{3}_{2}O_{3}$ values are significantly higher in unit 4. Most other major constituents (Appendix A) also follow a pattern of relatively constant concentrations in units 1 to 3, and significantly different values in unit 4. Similar patterns result from using only mean values from the 8 distal mesas in the Puye quadrangle (Fig. 5): TiO_2 levels are higher in units 2 and 3 than in unit 1, but most oxide concentrations overlap at the 2σ level in units 1g through 3.

Minor-element chemistry

Concentrations of trace elements analyzed using XRF and INAA techniques display more systematic variation than the major elements in UBT. Basal to upper-section enrichment

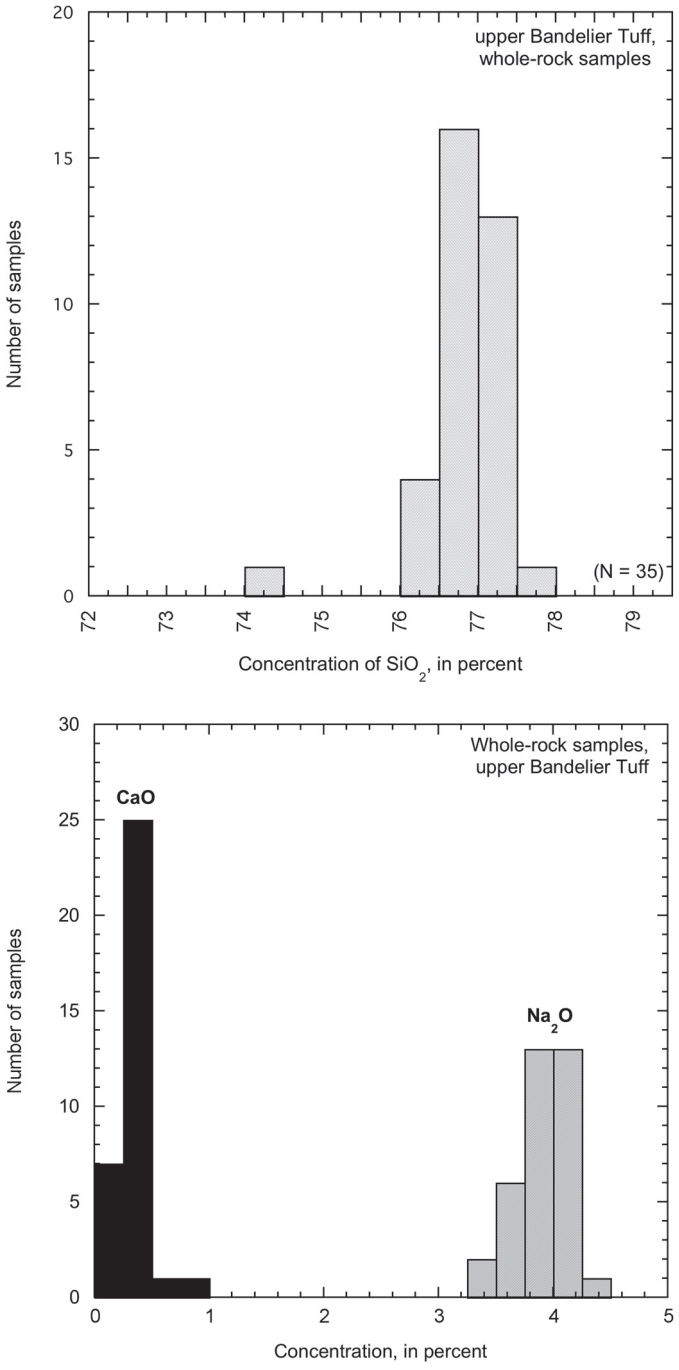

FIGURE 4. Distribution of SiO_2 (upper) and CaO and Na_2O (lower) concentrations in 35 whole-rock samples of Tshirege Tuff from Puye quadrangle mesas.

factors plotted for 18 trace elements (Fig. 6) show that values based on the composition of the Tsankawi Pumice bed and UBT4 (Tsankawi/UBT4) range from <0.5 (Ba and Eu) to values >3 for Cs and Rb and for uranium-group elements such as U, Ta and Yb. Plotted enrichment factors are <1 for Sc, Co and Ni as well, but the concentrations of these elements in the Tsankawi Pumice are not known with certainty. Thickness of the UBT and individual units generally decreases to the north and east (Fig. 1), but local thicknesses and field characteristics vary substantially (Fig. 7).

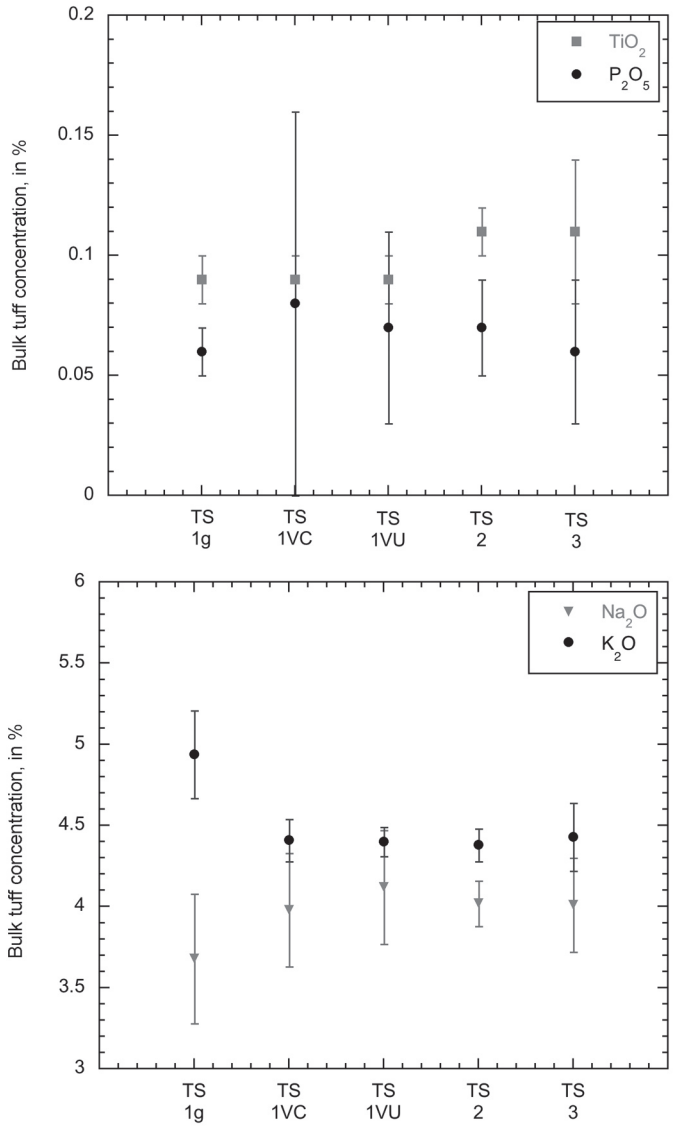

FIGURE 5. Plots showing concentration of TiO_2 and P_2O_5 (upper) and Na_2O and K_2O (lower) in units of the UBT. Mean and 2σ values for samples from Puye quadrangle mesas are plotted for units 1g (n=7), 1vc (n=8), 1vu (n=8), 2 (n=6), and 3 (n=5).

Multiple measurements from 10 sites indicate that concentrations of Eu, Sr and Zr in units 1 to 3 show little lateral or vertical variation across the area; Rb values vary more systematically in units 2 and 3 (Fig. 8). Unit 4 contains higher concentrations of these elements. Measurements at TA-21 suggest that concentrations of Rb, Sr and Zr are somewhat higher in the Tsankawi Pumice than in units 1 through 3.

Comparison of trace-element concentrations in stratigraphic sections at LANL and Puye mesas demonstrates that several groups of elements reflect similar patterns of zonation across the area. Plots of U and Yb (Fig. 9) show parallel trends at most mesas. Concentrations in units 1g, 1vc and 1vu are similar and higher than levels in units 2 and 3, which are comparable; unit 4 at TA-21 has the lowest values. Concentrations in the basal unit (1g) at 9 mesas generally are within 10% of the mesa mean value. However, the 1g and both 1v concentrations at Mesa 25 and the 1vc and 1vu concentrations at Mesa 19 are anomalous. Plots of both Rb and Cs (Fig. 10) reflect more variation in 1g values, but are otherwise similar to the pattern for Yb and U. Concentrations in units 1vc and 1vu, the devitrified equivalents of 1g, are mainly lower and less variable than in the basal unit. Patterns at Mesas 19 and 25 are similar to those for U and the Mesa 19 1vu value for both Rb and Cs is higher than all the values measured in units 2 and 3.

Zonation patterns of the divalent elements Zn and Ba are somewhat different from those portrayed at the other mesas and values at Mesas 19 and 25 are also anomalous (Fig. 11). Zn values in 1g and 1vc display little variation, but concentrations measured in 1vu are mainly higher and more variable than the 1vc values. Concentrations in unit 2 are substantially lower and fall within a restricted range; values in units 3 and 4 are somewhat lower. Ba concentrations (Fig. 11) increase upward, but concentrations are variable within each of the units and at each of the mesas. Concentrations measured in unit 3 are particularly variable. The single value plotted for unit 4 (TA-21) is considerably higher, but comparable to values measured at TA-67 (Appendix A).

DISCUSSION

The pattern of variation in minor elements from units of the upper Bandelier Tuff, together with previous work, demonstrates that the tuff sheets tapped a zoned magma chamber. Concentrations of major and minor elements in individual UBT units on the Pajarito Plateau do not show significant lateral variation across tens of kilometers. In vertical sections through the tuff, oxide data (Appendix A) show significant differences mainly between

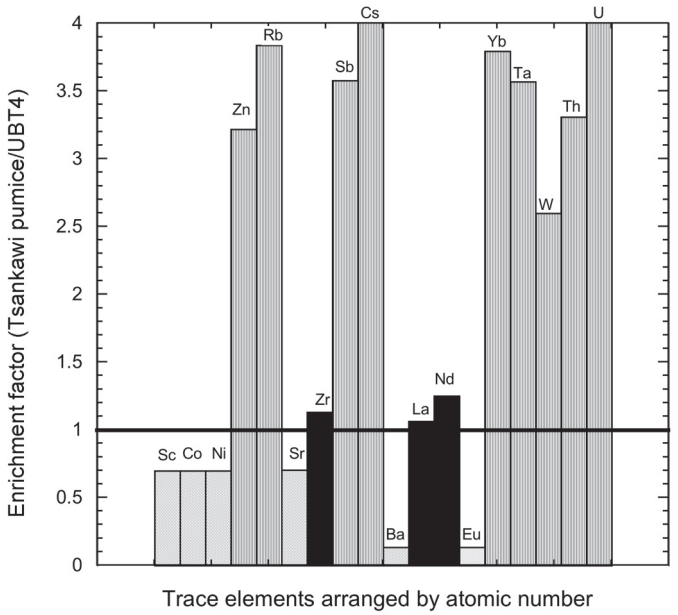

FIGURE 6. Enrichment factors (Concentration $_{\text{Tsankawi Pumice}}$/Concentration $_{\text{Tshirege Tuff unit 4}}$), for 18 minor elements plotted from low to high atomic number.

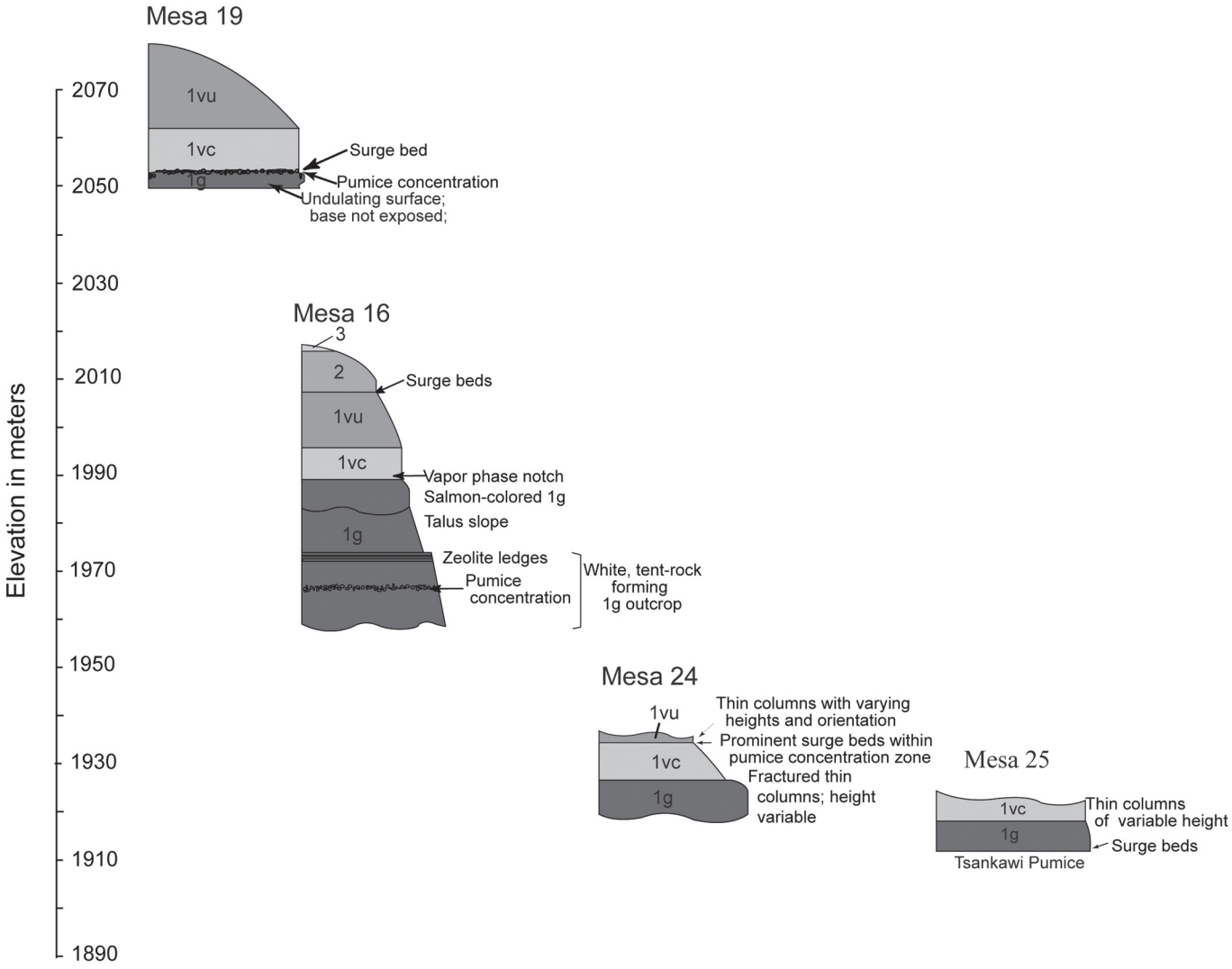

FIGURE 7. Stratigraphic sections showing UBT units and sample locations at mesas 19, 16, 24 and 25 (see Fig. 3).

the chemistry of unit 4 and that of units 1 to 3; TiO_2 concentrations apparently rise upsection above unit 1, a trend noted by Stimac et al. (2002) in the LANL area. Trace elements such as Cs, U and Zn in the same sections show a consistent pattern of zonation. Apparent concentration changes and patterns of relatively low versus high variance in the trace element content within UBT unit 1 may result from local mineralogic control or elemental redistribution during vapor-phase alteration. Trace element chemistry from tuff at Mesas 19 and 25 is anomalous, and suggests that field identification of the units may be incorrect or that other processes may affect trace-element zonation in the thinnest, distal tuffs.

Enrichment of most trace elements in early-erupted, glassy material (Tsankawi pumice; UBT unit 1) is typical of high-silica rhyolites (Wilson and Hildreth, 1997) and may reflect control by (1) gradients in the liquid fraction of the magma, perhaps controlled by complexing with Cl and other volatile components; (2) concentration of metals in the volatile phase; or (3) fractionation by alkali feldspar and phenocrysts of minor phases such as allanite. Enrichment is greatest for Cs and Sb and smallest for Eu, similar to patterns noted for the Bishop Tuff by Wilson and Hildreth (1997). In contrast to the Bishop Tuff, in which Sc is substantially enriched and Sr has a value of ~0.1, UBT Sc and Sr have enrichment factors ~0.7. Eu, Ba, and to a lesser degree Ni and Co are compatible with early-formed phenocrysts or matrix constituents such as Fe-Ti oxides, which may explain their relative enrichment in units 3 and 4. Figures 8 to 10 and some trace elements in Appendix A demonstrate a significant chemical change from unit 1 to 2 and suggest persistent differences between 2 and 4. Concentrations in unit 3 overlap with those in both 2 and 4. Trace-element data thus are consistent with surge deposits and other field evidence that suggests a temporal break between units 1 and 2 and a less well defined distinction between 2 and 3 (Broxton and Reneau, 1995). Unit 2 is widely distributed on the Pajarito Plateau, implying that its eruption tapped a deeper zone in the Valles magma chamber rather than a different area of the magma body.

Trace-element concentrations within unit 1 could be an artifact of sampling different amounts of fine glass, pumice fragments, phenocrysts and accidental fragments or could reflect postdepositional redistribution of elements. Plots of Cs and Rb, for

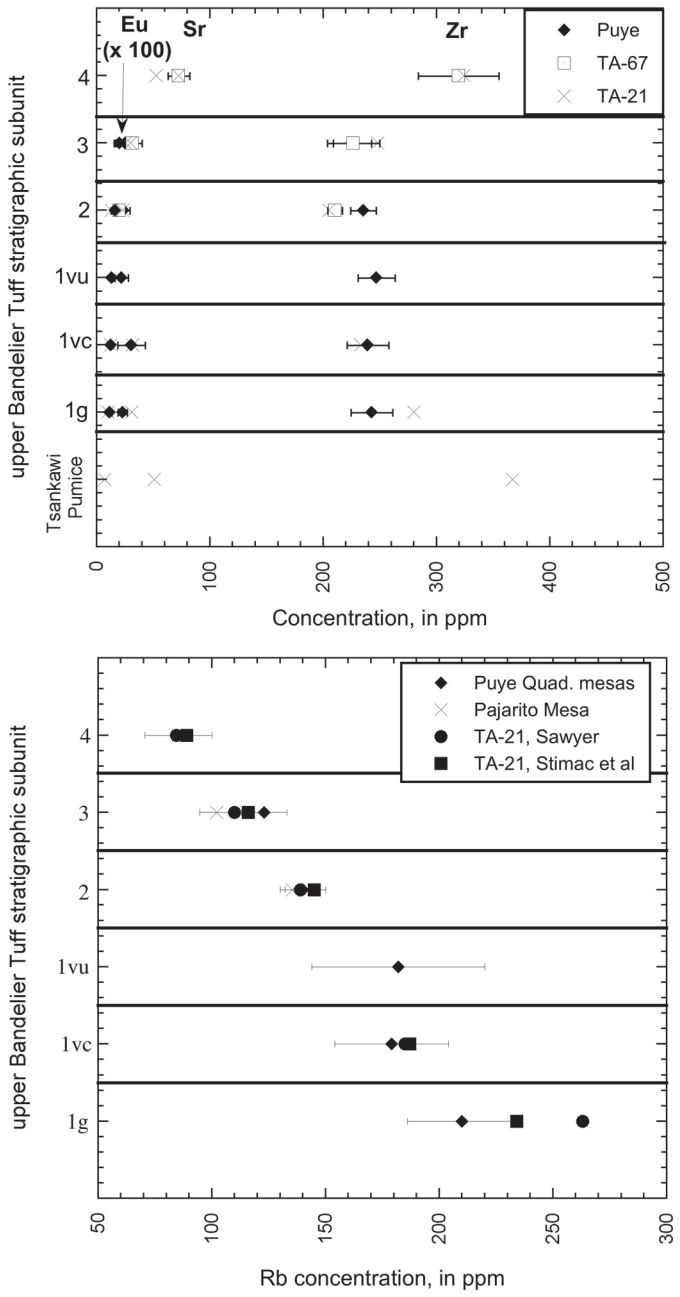

FIGURE 8. Plots showing concentration of Eu (X 100), Sr, and Zr (upper) and Rb (lower) in units of the UBT. Mean and 1σ values for samples from 8 Puye quadrangle mesas are plotted for units 1g (n=8), 1vc (n=8), 1vu (n=8), 2 (n=6), and 3 (n=5). Mean and 1σ values for TA-67 are calculated for multiple samples spaced at ~5 m intervals vertically (Broxton et al., 1995b) for the following units: 2 (n = 6); 3 (n=16); and 4 (n=3). Values for TA-21 are single samples.

instance, suggest that concentrations and variance decrease from 1g to 1vu. Values for Cs, which range from about 6 to 11 ppm in 1g and from about 4.8 to 5.8 ppm (excluding values from Mesas 19 and 25 and TA-21) in 1vu are particularly striking (Fig. 9). U and Yb do not change significantly in this interval. In contrast, Zn variance and concentrations apparently increase from 1g to 1vu. Variability in the more mobile elements (Cs, Rb, Zn) suggests that they may have been redistributed during the degassing and vapor-phase alteration that recrystallized unit 1 (Stimac et al., 1996).

Zonation of trace elements at Mesas 19 and 25 (Fig. 7) shows that what Dethier and Kampf (2007) mapped as units 1v and 1vc at both mesas and 1g at Mesa 25 have chemical characteristics typical of 2 or 3. Mesa 19 and nearby mesas (Fig. 3) have anomalously high, thick sections of 1v and thin sections of 1g compared to nearby areas. Having failed to locate surge deposits or other stratigraphic changes typical of the break between units 1 and 2, we interpret these field relations to mean that the preserved sec-

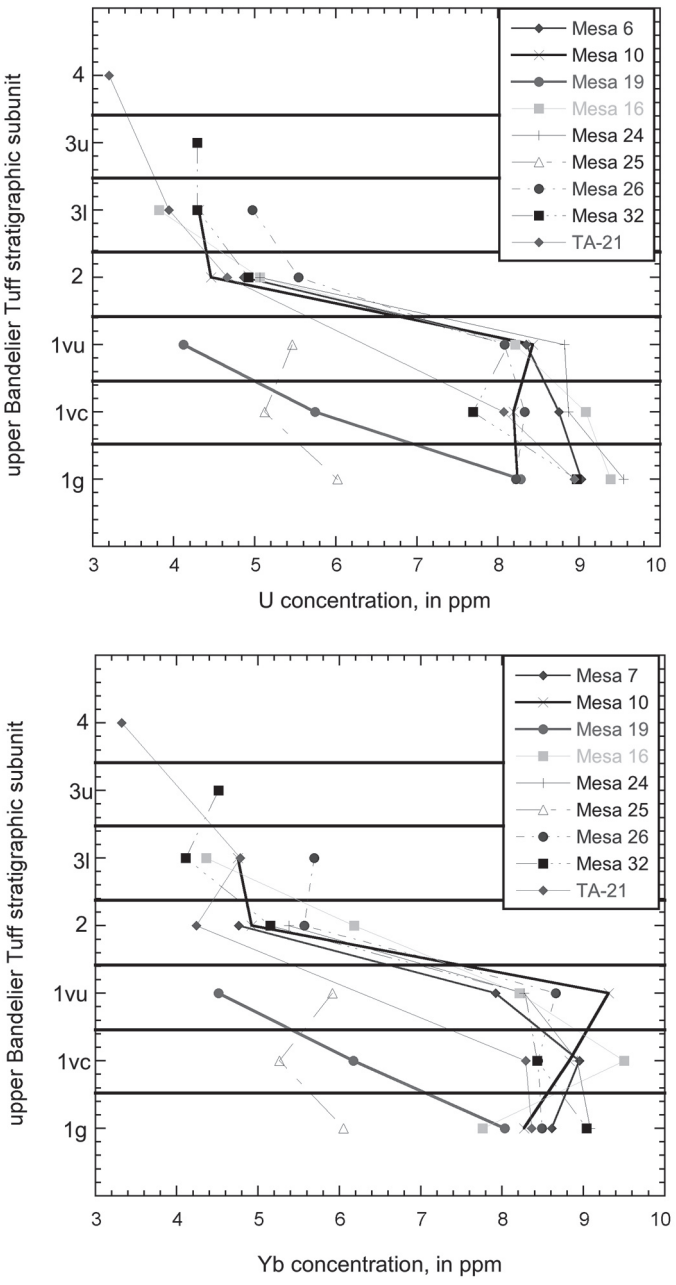

FIGURE 9. Plots showing concentration of elements measured in UBT units at nine stratigraphic sections. Upper = U; lower = Yb.

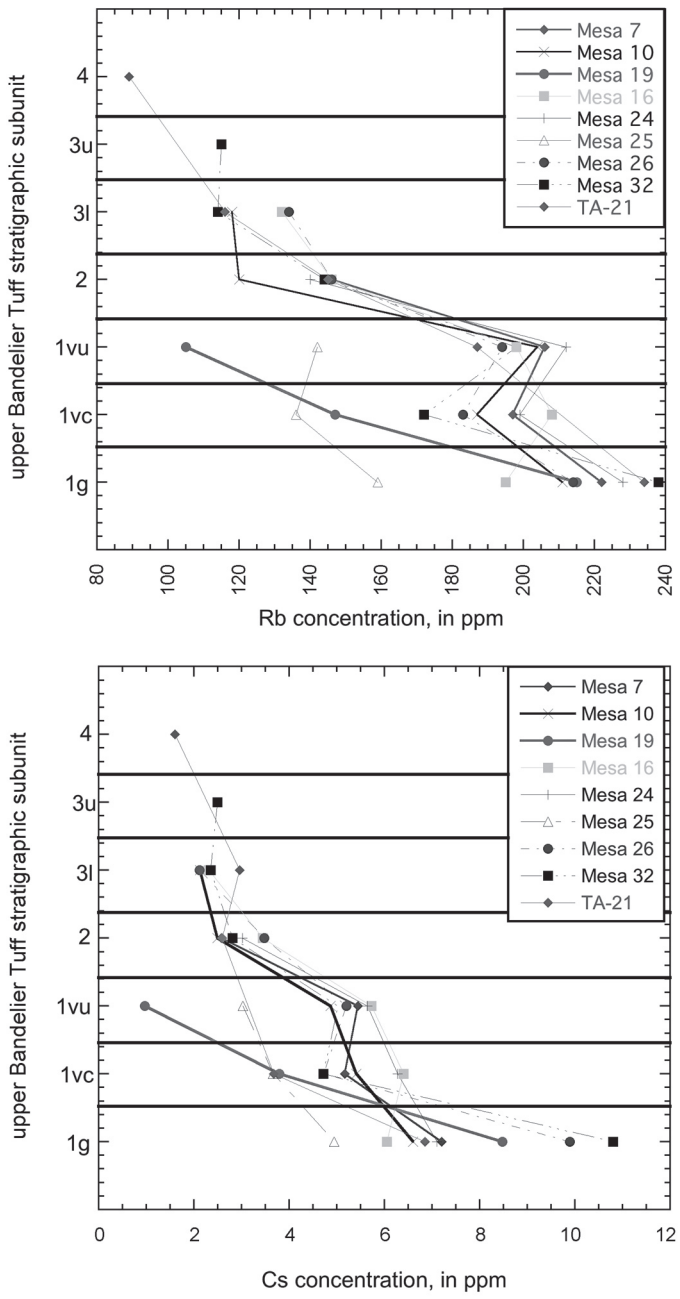

FIGURE 10. Plots showing concentration of elements measured in UBT units at nine stratigraphic sections. Upper = Rb; lower = Cs.

tion at Mesa 19 records only the final pyroclastic flows of unit 1. Trace-element chemistry, however, suggests that the mapped 1vc and 1vu are units 2 and 3, respectively, and that the surge bed mapped between 1g and 1vc actually represents the break between units 1 and 2 (Fig. 7). With the exception of the Ba concentration in 1g and 1vu, trace-element concentrations and zonation at Mesa 25, the most distal exposure of UBT on the Pajarito Plateau, do not correspond with any of the other patterns we have examined. Concentrations of trace elements at Mesa 24, which is nearly as distal as 25, generally fall at the upper or lower end of values plotted in Figures 8 to 10, but zonation is similar to that of the other mesas. Field relations suggest that Mesa 25 represents the topographically inverted fill of a narrow, early Pleistocene side canyon. The trace-element chemistry suggests that the sequence represents either (1) the upper part of a distal 1v through units 2 and 3, (2) tuff units we have not sampled elsewhere, or (3) an unusual pattern of elemental remobilization.

CONCLUSIONS

Outcrop morphology and the oxide and trace-element chemistry of upper Bandelier Tuff on the northeastern Pajarito Plateau

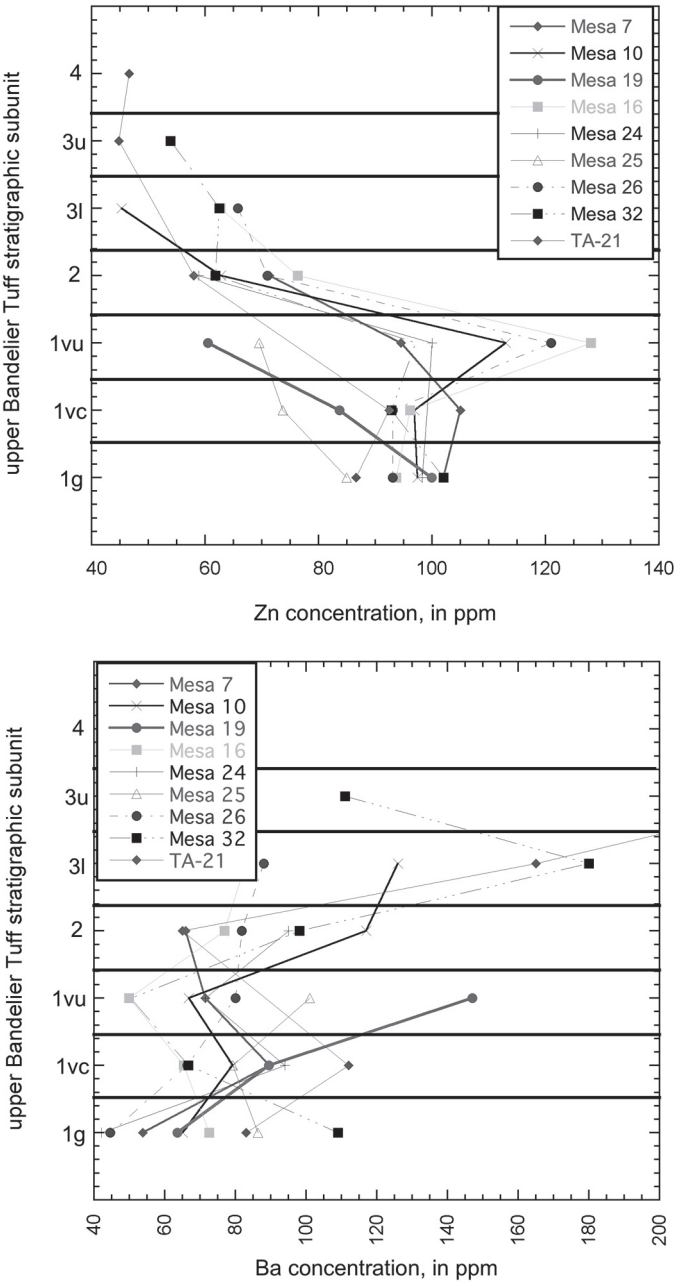

FIGURE 11. Plots showing concentration of elements measured in UBT units at nine stratigraphic sections. Upper = Zn; lower = Ba.

are similar to more completely studied proximal outcrops near Los Alamos, New Mexico. Lateral chemical variation of bulk tuff chemistry for units 1 through 4 is small. Vertical variations are relatively small for major oxides in units 1 through 3, but are more pronounced between units 3 and 4. Trace element chemistry displays significant chemical changes from unit 1 to 2 and suggests persistent differences between 2 and 4. Concentrations in unit 3 overlap with those in both 2 and 4. Trace-element data are thus consistent with field evidence that suggests a temporal break between units 1 and 2 and a less-well defined distinction between 2 and 3 (Broxton and Reneau, 1995). The pattern of trace-element differences suggests control of minor constituents by phenocrysts such as allanite and Fe-Ti oxides in a zoned magma chamber, and mobilization of certain elements such as Zn by vapor-phase alteration. Trace element chemistry from two mesas is anomalous and suggests that field identification of the units may be incorrect or that other processes may affect trace-element zonation in the thin, distal tuffs.

ACKNOWLEDGMENTS

This work was supported by the U. S. Geological Survey and by the Bronfman Science Center of Williams College. We gratefully acknowledge permission to conduct field work granted by San Ildefonso Pueblo and the logistical support offered to us by members of the Pueblo. David Broxton, Steve Reneau and Dave Vaniman of the Los Alamos National Laboratory provided field assistance, advice and an exhaustive knowledge of the field characteristics of Tshirege units. Vaniman and Bud Wobus provided valuable reviews of an earlier version of this paper.

REFERENCES

Broxton, D.E., and Eller, P.G., eds., 1995, Earth science investigations for environmental restoration--Los Alamos National Laboratory Technical Area 21: Los Alamos National Laboratory, Report LA-12934-MS, 118 p.

Broxton, D.E., and Reneau, S.L., 1995, Stratigraphic nomenclature of the Bandelier Tuff for the environmental restoration project at Los Alamos National Laboratory: Los Alamos National Laboratory, Report LA-13010-MS, 18 p.

Broxton, D.E., Heiken, G.H., Chipera, S.J., and Byers, F.M. Jr., 1995a, Stratigraphy, petrography, and mineralogy of Bandelier Tuff and Cerro Toledo deposits: Los Alamos National Laboratory, Report LA-12934-MS, p. 33-63.

Broxton, D.E., Vaniman, D., Chipera, S.J., Byers, F.M. Jr., Kluk, E.C., and Warren, R.G., 1995b, Stratigraphy, mineralogy and chemistry of bedrock tuffs at Pajarito Mesa: Los Alamos National Laboratory, Report LA-13089-MS, p. 5-30.

Budahn, J.R., and Wandless, G. A., 2002, Instrumental neutron activation analysis by long count, Chapter X, *in* Taggart, J.E. Jr., ed., Analytical methods for chemical analysis of geologic and other materials, U.S. Geological Survey, Open-File Report 02-223.

Dethier, D.P., and Kampf, S.K., 2007, Reconstructing pyroclastic flow dynamics and landscape evolution using the upper Bandelier Tuff, Puye quadrangle, New Mexico: New Mexico Geological Society, 58th Field Conference Guidebook, p. 344-353.

Reneau, S.L., and Raymond, R. Jr., eds., 1995, Geological site characterization for the proposed mixed waste disposal facility, Los Alamos National Laboratory: Los Alamos National Laboratory, Report LA-13089-MS, 100 p.

Rogers, M.A., 1995, Geologic map of Los Alamos National Laboratory Reservation: State of New Mexico Environment Department, scale 1:400.

Sarna-Wojcicki, A.M., and Davis, J.O., 1991, Quaternary tephrochronology, *in* Morrison, R.B., ed., Quaternary nonglacial geology; conterminous U.S.: Boulder, Colorado, Geological Society of America, The Geology of North America, v. K-2, p. 93-116.

Smith, R.L., and Bailey, R.A., 1966. The Bandelier Tuff: A study of ash-flow eruption cycles from zoned magma chambers. Bulletin of Volcanology, v. 29, p. 83–104.

Stimac, J., Hickmott, J., Abell, R., Larocque, A.C.L., Broxton, D.E., Gardner, J., Chipera, S., Wolff, J., and Gaueke, E., 1996, Redistribution of Pb and other volatile trace metals during eruption, devitrification, and vapor-phase crystallization of the Bandelier Tuff, New Mexico." Journal of Volcanology and Geothermal Research, v. 73, p. 245-266.

Stimac, J.A., Broxton, D.E., Kluk, E.C., Chipera, S.J., and Budahn, J.R., 2002, Stratigraphy of the tuffs from Borehole 49-2-700-1 at Technical Area 49, Los Alamos National Laboratory, New Mexico: Los Alamos National Laboratory, Report LA-13969-MS, 46 p.

Taggart, J.E. and Siems, D.F., 2002, Major element analysis by wavelength dispersive x-ray fluorescence spectrometry, *in* Taggart, J.E. Jr., ed., Analytical methods for chemical analysis of geologic and other materials, U.S. Geological Survey, Open-File Report 02-223, Chapter "T", 13 p.

Wilson, C.J.N., and Hildreth, W., 1997, The Bishop Tuff: New insights from eruptive stratigraphy: Journal of Geology, v. 105, p. 407–439

APPENDIX A. Selected chemical analyses from units of the upper Bandelier Tuff in the Puye quadrangle and adjacent areas.

					Values by x-ray fluorescence																					
FIELD NUMBER	Mesa Location	Latitude	Longitude	Elevation	SiO2 %	Al2O3 %	FeTO3 %	MgO %	CaO %	Na2O %	K20 %	TiO2 %	P2O5 %	MnO %	LOI,925C %	Total %	runno	Fe %	Ca %	Na %	K %	Rb ppm	Sr ppm	Cs ppm	Ba ppm	Th ppm	U ppm
SKN97-C-2L	7	35°56'.6 N	106°13'.2 W	6815'	77.36	11.86	1.44	0.09	0.2	4.1	4.44	0.1	0.07	0.06	0.18	99.72	NDL373	1	0.3	3.15	3.6	146	15	2.58	65.9	17.8	4.86
SKN97-C-1VU	7	35°56'.6 N	106°13'.2 W	6780'	76.77	12	1.48	0.09	0.17	4.24	4.46	0.09	0.07	0.07	0.58	99.44	NDL373	1.03	0.16	3.22	3.63	206	20.1	5.44	71.4	26.5	8.35
SKN97-C-1VC	7	35°56'.6 N	106°13'.2 W	6755'	76.3	12.38	1.51	0.05	0.29	3.93	4.54	0.08	0.18	0.08	0.81	99.35	ndl394	1.04	0.08	3.05	3.69	197	16.4	5.17	89.6	26.2	8.75
SKN97-C-1G	7	35°56'.6 N	106°13'.2 W	6739'	76.54	12.07	1.54	0.05	0.27	3.81	4.84	0.08	0.06	0.08	2.15	99.35	NDL373	1.05	0.35	2.82	3.8	222	23.1	7.2	53.8	27.5	9.03
SKN97-D-3S	10	35°55'.8 N	106°14'.6 W	7132'	76.96	11.78	1.39	0.08	0.74	4.04	4.36	0.12	0.07	0.04	0.71	99.58	NDL373	0.99	0.83	3.13	4.9	118	21.2	2.13	126	15.1	4.31
SKN97-D-2L	10	35°55'.8 N	106°14'.6 W	7098'	77.37	11.84	1.5	0.11	0.34	4.04	4.37	0.12	0.07	0.05	0.28	99.82	NDL373	1.01	0.26	3.07	3.41	120	21.8	2.49	117	15.2	4.46
SKN97-D-1VU	10	35°55'.8 N	106°14'.6 W	7080'	76.69	11.94	1.52	0.09	0.42	4.21	4.44	0.09	0.09	0.08	0.97	99.58	NDL373	1.09	0.37	3.25	3.92	204	33.1	4.87	66.8	26.3	8.43
SKN97-D-1VC	10	35°55'.8 N	106°14'.6 W	7065'	76.77	11.8	1.45	0.05	0.39	3.94	4.42	0.08	0.06	0.08	0.91	99.04	ndl394	0.99	0.2	3.02	3.39	187	48.2	5.41	79.2	24.3	8.19
SKN97-D-1G	10	35°55'.8 N	106°14'.6 W	7052'	76.9	11.56	1.46	0.08	0.35	3.65	5.15	0.09	0.07	0.08	1.84	99.39	NDL373	1.02	0.54	2.73	4.64	211	18.3	6.6	65.1	23.7	8.24
SKN97-F-1VU	19	35°55'.1 N	106°12'.6 W	6818'	77.15	11.43	1.31	0.43	0.85	3.74	4.31	0.1	0.07	0.06	1.17	99.46	ndl394	0.9	0.07	2.84	3.71	105	19.7	0.97	147	14.2	4.12
SKN97-F-1VC	19	35°55'.1 N	106°12'.6 W	6738'	77.06	11.89	1.44	0.05	0.25	3.9	4.41	0.1	0.08	0.06	0.69	99.25	ndl394	1	0.09	3.04	3.48	147	14.9	3.79	89.5	18.2	5.74
SKN97-F-1G	19	35°55'.1 N	106°12'.6 W	6726'	76.5	11.78	1.53	0.05	0.37	3.52	5.11	0.09	0.06	0.07	1.87	99.07	ndl394	1	0.09	2.7	4.37	215	28.5	8.48	63.6	23.4	8.28
SKN97-G-3S	16	35°55'.4 N	106°11'.5 W	6714'	77.41	11.75	1.36	0.05	0.26	3.88	4.36	0.1	0.05	0.06	0.05	99.27	ndl394	0.94	0.8	3	3.16	132	26.9	2.31	82.9	16.4	3.82
SKN97-G-2L	16	35°55'.4 N	106°11'.5 W	6693'	77.03	11.76	1.46	0.05	0.27	3.94	4.35	0.11	0.06	0.06	0.19	99.08	ndl394	0.99	0.31	3.07	3.07	146	18.6	3.44	76.9	18	5.06
SKN97-G-1VU	16	35°55'.4 N	106°11'.5 W	6670'	76.85	11.98	1.53	0.05	0.34	4.06	4.38	0.09	0.06	0.08	0.85	99.42	ndl394	0.98	0.2	3.08	3.17	198	20.3	5.73	49.9	24.1	8.21
SKN97-G-1VC	16	35°55'.4 N	106°11'.5 W	6656'	76.8	11.92	1.43	0.05	0.31	4.01	4.4	0.09	0.07	0.07	0.68	99.15	ndl394	0.98	0.09	3.11	3.57	208	39	6.4	65.4	25.5	9.08
SKN97-G-1G (2)	16	35°55'.4 N	106°11'.5 W	6515'	74.31	11.22	1.45	0.35	3.86	3.82	4.21	0.09	0.19	0.08	5.2	99.57	ndl394	0.93	2.16	2.77	3.5	195	134	6.05	72.6	22.7	9.39
SKN97-J-2L	24	35°54'.8 N	106° 9'.8 W	6358'	77.28	11.77	1.42	0.06	0.21	3.95	4.4	0.1	0.07	0.05	0.33	99.32	NDL373	1	0.22	3.07	3.71	140	27.5	3.02	95	17.3	5.06
SKN97-J-1VU	24	35°54'.8 N	106° 9'.8 W	6347'	76.94	11.86	1.52	0.06	0.2	4.24	4.38	0.09	0.06	0.07	0.75	99.43	NDL373	1.07	0.23	3.22	3.81	212	14.9	5.64	71.5	26.4	8.82
SKN97-J-1VC	24	35°54'.8 N	106° 9'.8 W	6328'	76.51	12.03	1.5	0.05	0.32	4.4	4.36	0.09	0.06	0.08	1.29	99.4	ndl394	1.02	0.1	3.42	3.31	199	41	6.28	94	25.3	8.87
SKN97-J-1G	24	35°54'.8 N	106° 9'.8 W	6322'	76.56	12.02	1.56	0.06	0.27	3.97	4.77	0.08	0.06	0.07	2.24	99.41	NDL373	1.06	0.18	3	4.16	228	17.9	7.1	42.1	27.1	9.55
SKN97-K-1VU	25	35°55'.4 N	106° 8'.8 W	6319'	76.84	11.74	1.44	0.07	0.24	4.05	4.41	0.1	0.06	0.06	0.32	99.02	NDL373	1.02	0.29	3.11	3.66	142	27.5	3.03	101	17.3	5.46
SKN97-K-1VC	25	35°55'.4 N	106° 8'.8 W	6316'	76.9	11.83	1.44	0.05	0.32	3.9	4.45	0.1	0.06	0.06	0.36	99.11	ndl394	0.98	0.36	3.03	3.7	136	32.1	3.66	79.3	17	5.12
SKN97-K-1G	25	35°55'.4 N	106° 8'.8 W	6285'	77.4	11.37	1.46	0.06	0.35	3.35	4.9	0.1	0.06	0.06	1.9	99.12	NDL373	1.01	0.25	2.47	4.25	159	19.5	4.94	86.4	18.6	6.02
SKN97-L-3S	26	35°54'.4 N	106°14'.6 W	7020'	77.35	11.87	1.45	0.08	0.27	4.1	4.43	0.1	0.07	0.06	0.38	99.77	NDL373	1.02	0.4	3.11	3.43	134	15.3	2.12	88	17.2	4.97
SKN97-L-2L	26	35°54'.4 N	106°14'.6 W	6958'	76.86	11.76	1.45	0.07	0.3	4.09	4.41	0.11	0.09	0.05	0.29	99.21	NDL373	1.03	0.24	3.18	4.13	146	29.6	3.48	81.8	18.6	5.54
SKN97-L-1VU	26	35°54'.4 N	106°14'.6 W	6937'	76.47	12.03	1.5	0.1	0.43	4.26	4.44	0.1	0.11	0.08	0.86	99.53	NDL373	1.08	0.44	3.22	3.48	194	17.4	5.2	80	24.5	8.08
SKN97-L-1VC	26	35°54'.4 N	106°14'.6 W	6923'	77.24	11.77	1.49	0.05	0.34	3.95	4.37	0.08	0.05	0.07	0.63	99.41	ndl394	1.03	0.27	3.05	4.18	183	21.9	4.72	66.4	24.7	8.33
SKN97-L-1G	26	35°54'.4 N	106°14'.6 W	6903'	77.02	11.68	1.51	0.05	0.34	3.72	4.89	0.09	0.06	0.07	2.13	99.44	NDL373	1.02	0.27	2.78	4.06	214	25.5	9.89	44.6	23.9	8.22
SKN97-M-3S	32	35°53'.3 N	106°14'.6 W	6880'	77.34	11.82	1.48	0.05	0.36	3.84	4.38	0.11	0.05	0.06	0.46	99.51	ndl394	0.95	0.16	2.85	3.86	115	23.5	2.49	111	14.5	4.29
SKN97-M-3L	32	35°53'.3 N	106°14'.6 W	6850'	76.09	12.37	1.62	0.1	0.37	4.18	4.61	0.14	0.08	0.07	0.7	99.64	NDL373	1.14	0.27	3.23	3.78	114	39.1	2.35	180	14.9	4.29
SKN97-M-2L	32	35°53'.3 N	106°14'.6 W	6821'	77.79	11.58	1.42	0.06	0.27	3.97	4.31	0.1	0.07	0.05	0.6	99.62	NDL373	1.07	0.26	3.15	3.68	144	26.5	2.81	98.1	20.8	4.92
SKN97-M-1VU	32	35°53'.3 N	106°14'.6 W	6770'	76.82	11.97	1.49	0.05	0.23	4.17	4.39	0.08	0.06	0.07	0.41	99.32	NDL373	1.06	0.29	3.22	4.03	198	19.1	5.03	50.2	23.1	8.13
SKN97-M-1VC	32	35°53'.3 N	106°14'.6 W	6718'	77.2	11.8	1.4	0.05	0.22	3.84	4.35	0.08	0.05	0.07	0.51	99.08	ndl394	0.98	0.4	3	3.08	172	27.9	4.72	66.7	22.5	7.69
SKN97-M-1G	32	35°53'.3 N	106°14'.6 W	6700'	76.47	12.26	1.57	0.06	0.38	3.71	4.9	0.1	0.07	0.07	2.08	99.59	NDL373	1.11	0.36	2.77	3.58	238	24.9	10.8	109	25.5	8.97
UBT4	TA-67																	1.48	0.46	3.13	4.52	84.4	72.1	1.6	332	12.2	3.2
UBT3	TA-21																	1.13	0.41	2.99	3.71	110	25.3	2.96	160	14.6	3.94
lsr pu	Tsank. pum bed																	1.47	0.83	2.7	3.27	196	189	6.23	361	24	8.73
UB3 lsr pu	Ponderosa Est.																	1.2	0.55	1.94	4.65	123	37.3	2.99	133	17	5.1
UBT3	Ponderosa Est.																	0.81	0.2	2.03	3.68	125		3.25	65.1	15.3	4.94
UBT3 pu	Ponderosa Est.																	1.02	0.23	2.24	3.26	103	29.2	2.47	154	13.4	3.92
UBT2	TA-21																	1.01	0.27	2.98	3.37	139	23	2.59	71.6	15.6	4.66
UBT1v	TA-21																	1.06	0.19	2.97	3.44	185	31.7	3.68	109	23.3	8.07
UBT1g	TA-21																	1.04	0.25	2.8	3.66	221		6.85	55.8	25.4	8.94
UBT1g	TA-21																	1.05	0.3	2.62	3.98	305	30.8	15.4	64.9	32.2	12.6
UBT1g pu	Pajarito Canyon																	1.09	0.24	2.41	5.34	290	24	9.56	48.2	34.1	13.2
UBTskpus	Tsank. pum bed																	1.14	0.52	2.84	3.64	290	33.7	9.85	41.6	35.3	13.6
Qbt3?	Ponderosa Estates																	1	0.54	1.94	3.94	188	43.3	5.3	40.7	24	7.81
Qbt1	Pajarito Canyon																	1.08	0.58	2.35	4.79	320	50.8	10.9	24.5	38.7	14.9
Qbt1	TA-21																	0.96	0.81	2.5	4.18	349	59.6	17.1	21.6	38	14.4
Tsankawi	Tsank. pum bed ?																	1.17	0.67	2.89	4.03	324	50.8	11.4	45.1	40.4	15.3

(1) Concentrations of elements by INAA except where noted

(2) Ca and Mg values from sample SKN97-G-1G suggest contamination with calcite; these values are not included in our calculations

La ppm	Ce ppm	Nd ppm	Sm ppm	Eu ppm	Gd ppm	Tb ppm	Ho ppm	Tm ppm	Yb ppm	Lu ppm	Zr ppm	Hf ppm	Ta ppm	W ppm	Sc ppm	Cr ppm	Co ppm	Ni ppm	Zn ppm	As ppm	Sb ppm	Au ppb	La ppm	Ce ppm	Nd ppm	Sm ppm	Eu ppm	Gd ppm	Tb ppm	Ho ppm	Tm ppm	Yb ppm	Lu ppm
46	106	34.1	7.76	0.12	7.37	1.19	1.7	0.77	4.76	0.69	221	7.87	5.37	1.68	1.11	1.26	0.47	3.71	71.3	1.02	0.16	1.62	147.91	130.38	56.46	39.59	1.66	28.35	25.32	23.68	23.65	22.67	21.3
53.7	122	46.3	11.8	0.11	11.3	2.04	2.96	1.27	7.92	1.11	253	9.8	8.27	3.42	1.08	2.04	1.34	3.92	94.5	2.08	0.37	1.99	172.67	150.06	76.66	60.2	1.53	43.46	43.4	41.23	38.96	37.71	34.37
56.3	116	50.2	13.3	0.12	13.7	2.37	3.33	1.39	8.95	1.24	255	9.46	8.5	4.18	1.14	1.21	0.59	3.86	105	2.3	0.36	0.1	181.03	142.68	83.11	67.86	1.66	52.69	50.43	46.38	42.64	42.62	38.39
57	119	48	12.4	0.09	11.8	2.17	3.15	1.36	8.61	1.21	250	10.1	8.63	4.66	1.05	0.11	0.36	7.62	102	2.61	0.37	1.1	183.28	146.37	79.47	63.27	1.26	45.38	46.17	43.87	41.72	41	37.46
53.6	112	40.5	8.59	0.25	7.53	1.27	1.77	0.74	4.75	0.69	221	7.09	4.16	1.84	1.32	0.94	0.66	4.32	45.3	1.14	0.16	2.48	172.35	137.76	67.05	43.83	3.45	28.96	27.02	24.65	22.61	22.62	21.24
60.7	110	48.4	10.2	0.25	8.45	1.42	1.94	0.81	4.92	0.73	253	7.76	4.14	2.03	1.43	2.24	0.63	4.36	62.8	1.14	0.16	1.47	195.18	135.3	80.13	52.04	3.36	32.5	30.21	27.02	24.94	23.43	22.54
59.2	120	52.9	13.8	0.14	13.5	2.44	3.52	1.48	9.31	1.32	261	9.84	8.41	4.32	1.17	1.26	0.91	5.05	113	2.26	0.38	2.94	190.35	147.6	87.58	70.41	1.91	51.92	51.91	49.03	45.4	44.33	40.87
52.6	111	48.1	13.1	0.12	14	2.38	3.29	1.44	8.83	1.23	249	9.49	7.77	4.12	1.04	0.5	0.55	1.73	96.9	2.35	0.35	0.66	169.13	136.53	79.64	66.84	1.58	53.85	50.64	45.82	44.17	42.05	38.08
52.2	106	46.2	12	0.1	12.2	2.1	3.27	1.33	8.27	1.17	231	8.93	7.7	4.72	0.99	1.15	0.49	3.81	97.4	2.2	0.36	1.75	167.85	130.38	76.49	61.22	1.35	46.92	44.68	45.54	40.8	39.38	36.22
50.2	99.8	38.8	8.62	0.16	8.01	1.29	1.97	0.73	4.51	0.64	212	6.79	3.97	2.11	1.15	0.41	0.64	3.27	60.5	1.31	0.26	0.71	161.41	122.76	64.24	43.98	2.15	30.81	27.45	27.44	22.27	21.48	19.69
57.2	109	48	11.3	0.16	10.3	1.7	2.14	0.99	6.17	0.84	215	7.5	5.39	2.61	1.19	0.81	0.51	1.9	83.7	2.3	0.32	1.99	183.92	134.07	79.47	57.65	2.19	39.62	36.17	29.81	30.4	29.38	26.13
51.3	107	44	11.9	0.09	12	2.12	2.92	1.31	8.03	1.13	234	8.96	7.52	4.37	1.03	1.63	0.38	1.63	99.9	2.14	0.46	0.92	164.95	131.61	72.85	60.71	1.28	46.15	45.11	40.67	40.18	38.24	34.98
54.8	105	41.3	8.78	0.14	7.38	1.23	1.52	0.71	4.36	0.63	212	6.99	4.69	1.07	1.07	0.07	0.46	1.99	62.7	1.06	0.13	1.36	176.21	129.15	68.38	44.8	1.91	28.38	26.17	21.17	21.75	20.76	19.54
59.5	114	49.3	11.4	0.14	10.4	1.74	2.45	0.98	6.18	0.89	236	7.86	5.26	1.59	1.14	0.7	0.41	1.29	76.3	1.14	0.2	0.1	191.32	140.22	81.62	58.16	1.92	40	37.02	34.12	30	29.43	27.43
55.3	113	46.9	12.4	0.11	12.6	2.15	3.09	1.28	8.21	1.1	247	9.18	7.52	3.34	1.09	0.09	0.39	1.74	128	1.84	0.28	1.2	177.81	138.99	77.65	63.27	1.43	48.46	45.74	43.04	39.26	39.1	34.06
55.8	113	51.2	14	0.11	14.8	2.5	3.86	1.54	9.5	1.28	254	9.62	8.34	3.7	1.04	0.5	0.4	1.64	96.1	3.44	0.42	1.54	179.42	138.99	84.77	71.43	1.53	56.92	53.19	53.76	47.24	45.24	39.63
46	96.1	40.7	11	0.11	11.6	1.96	3.01	1.2	7.76	1.06	221	8.55	7.44	5.3	1.01	0.98	0.54	1.38	93.7	3.32	0.39	0.61	147.91	118.2	67.38	56.12	1.42	44.62	41.7	41.92	36.81	36.95	32.82
61.1	116	47.8	10.5	0.16	9	1.53	2.22	0.84	5.38	0.77	226	7.47	4.94	2.22	1.17	0.74	0.38	6.47	58.9	1.31	0.18	2.54	196.46	142.68	79.14	53.57	2.09	34.62	32.55	30.92	25.8	25.62	23.84
54.2	115	46.6	12.1	0.1	10.8	2.07	3.13	1.3	8.27	1.15	251	9.85	8.42	4.31	0.93	0.92	0.59	6.38	100	1.91	0.29	2.64	174.28	141.45	77.15	61.73	1.36	41.54	44.04	43.59	39.88	39.38	35.6
54.2	113	48.3	13	0.12	13.5	2.35	3.49	1.39	8.92	1.2	255	9.64	8.24	4.37	1.24	0.81	0.4	1.92	264	2.03	0.32	1.62	174.28	138.99	79.97	66.33	1.68	51.92	50	48.61	42.64	42.48	37.15
55.3	119	48.1	13	0.1	13.3	2.29	3.33	1.45	9.08	1.26	278	10.3	8.88	5.4	1.02	0.8	0.43	4.28	98.3	2.31	0.36	2.79	177.81	146.37	79.64	66.33	1.3	51.15	48.72	46.38	44.48	43.24	39.01
58.6	112	47.4	10.5	0.14	10.1	1.62	2.35	0.96	5.91	0.85	238	7.83	5.16	2.02	1.17	0.25	0.49	4.74	69.5	1.13	0.18	2.85	188.42	137.76	78.48	53.57	1.95	38.85	34.47	32.73	29.54	28.14	26.44
56.4	110	44.1	9.95	0.13	8.79	1.47	2.14	0.8	5.26	0.73	209	7.24	5	2.6	1.17	0.46	0.38	2.89	73.7	1.27	0.19	1.53	181.35	135.3	73.01	50.77	1.8	33.81	31.28	29.81	24.45	25.05	22.66
56.5	114	46.8	10.6	0.13	10.2	1.63	2.4	0.96	6.05	0.86	229	7.94	5.55	3.51	1.15	0.48	0.43	4.21	84.9	1.85	0.25	22.6	181.67	140.22	77.48	54.08	1.78	39.23	34.68	33.43	29.36	28.81	26.56
62.6	114	50.9	11.2	0.19	10.1	1.66	2.23	0.94	5.69	0.81	237	7.79	4.82	1.45	1.32	1.91	0.61	5.32	65.8	1.03	0.16	1.66	201.29	140.22	84.27	57.14	2.58	38.85	35.32	31.06	28.83	27.1	25.05
58	110	45.4	10	0.14	9.06	1.51	2.2	0.92	5.57	0.8	240	7.99	5.26	2.46	1.12	0.23	0.45	5.25	71	1.33	0.21	1.17	186.5	135.3	75.17	51.02	1.95	34.85	32.13	30.64	28.28	26.52	24.86
58.3	119	51.2	13	0.14	13.1	2.24	3.25	1.35	8.66	1.22	264	9.55	7.7	3.48	1.24	0.81	0.69	8.84	121	1.66	0.36	1.87	187.46	146.37	84.77	66.33	1.85	50.38	47.66	45.26	41.41	41.24	37.77
56.9	119	51.3	13.1	0.12	13	2.25	3.19	1.33	8.44	1.18	232	9.21	7.69	4	1.18	0.42	0.34	4.2	93.1	2.53	0.37	1.44	182.96	146.37	84.93	66.84	1.64	50	47.87	44.43	40.8	40.19	36.53
55.6	113	48	12.8	0.1	12.7	2.21	3.16	1.33	8.49	1.19	239	9.14	7.6	4.69	0.97	0.13	0.29	6.39	93.1	1.95	0.34	1.33	178.78	138.99	79.47	65.31	1.36	48.85	47.02	44.01	40.8	40.43	36.84
54.7	101	42.6	9.1	0.18	7.99	1.28	1.62	0.67	4.51	0.65	208	6.8	4.01	1.3	1.2	1.16	0.49	2.6	53.9	1.54	0.14	3.19	175.88	124.23	70.53	46.43	2.41	30.73	27.23	22.56	20.46	21.48	20.25
58.3	118	41.5	8.17	0.25	6.81	1.06	1.54	0.66	4.11	0.6	248	7.56	4.05	1.41	1.69	0.54	1	4.93	62.5	1.52	0.15	1.33	187.46	145.14	68.71	41.68	3.39	26.19	22.55	21.45	20.18	19.57	18.73
52.6	132	39.8	8.62	0.16	8.9	1.31	1.91	0.82	5.15	0.75	234	8.14	5.11	1.02	1.35	1.19	0.67	4.58	61.8	1.24	0.16	1.95	169.13	162.36	65.89	43.98	2.2	34.23	27.87	26.6	25.18	24.52	23.07
58.4	117	52.4	13.2	0.11	12.9	2.2	3.13	1.28	8.28	1.17	247	9.23	7.65	2.97	1.11	0.38	0.38	5.42	97.1	2.06	0.33	1.62	187.78	143.91	86.76	67.35	1.42	49.62	46.81	43.59	39.26	39.43	36.22
56.6	107	51.3	13.5	0.1	13.9	2.28	3.32	1.31	8.43	1.19	241	8.8	7.48	4.27	0.98	0.62	0.29	2.74	92.9	2.33	0.32	1.39	181.99	131.61	84.93	68.88	1.41	53.46	48.51	46.24	40.18	40.14	36.84
56.2	113	49	13	0.14	13.1	2.28	3.29	1.45	9.04	1.28	257	9.94	8.4	4.36	1.16	1.54	0.54	4.47	102	2.51	0.37	2.51	180.71	138.99	81.13	66.33	1.95	50.38	48.51	45.82	44.48	43.05	39.63
61	119	40.8	7.14	0.52	5.64	0.86	1.24	0.54	3.32	0.49	324	8.68	4.23	84	2.56	2.36	21.9	7.79	46.6	1.3	0.19												
61.3	121	46.9	10	0.3	8.93	1.35	1.85	0.82	4.78	0.69	248	7.34	5.72	121	1.9	2.02	13	5.02	44.8	1.45	0.26												
55.3	110	47.2	12.4	0.35	13.2	2.02	2.86	1.26	8.23	1.17	300	10.7	8.38	5.11	2.27	3.95	2.81	3.5	97.6	2.31	0.36												
60.6	119	49.3	10.9	0.32	10.1	1.45	1.97	0.82	5.24	0.75	261	8.13	4.92	3.19	1.67	3.47	3.97	8.49	59.2	1.48	0.26												
51.8	103	42	9.62	0.13	8.82	1.37	1.86	0.79	4.94	0.71	196	6.71	4.56	4.13	0.92	1.21	1.21	2.1	55.3	2.4	0.28												
60.8	113	45.6	9.21	0.28	8.02	1.17	1.67	0.7	4.18	0.61	249	7.29	3.64	1.29	1.49	1.09	3.88	8.86	51.9	0.89	0.16												
40.5	88.3	29.5	6.63	0.13	6.14	1.01	1.5	0.67	4.24	0.61	205	7.32	7.84	163	1.14	1.12	12.2	1.33	58	0.69	0.13												
55.3	112	50.4	13.4	0.13	14.2	2.23	3.16	1.41	8.29	1.16	233	8.78	10.3	168	1.28	1.25	14.4	5	92.4	2.31	0.49												
52	107	43.3	11.7	0.1	12.5	2.07	3.01	1.37	8.36	1.16	243	9.6	10.5	120	1.06	1.08	13.8	1.25	86.6	2.34	0.34												
57.1	123	53.5	14.7	0.06	16.2	2.56	3.89	1.73	10.9	1.53	314	12.6	11.5	6.5	0.72	0.8	0.94	2.58	117	2.97	0.43												
57.6	123	49.2	13.9	0.05	15.4	2.58	3.95	1.78	11.4	1.6	291	13	12.5		0.71	0.42	0.67	6.94	122	3.44	0.5												
57.7	120	49.5	13.9	0.07	15.9	2.57	4.01	1.8	11.7	1.63	330	13.8	13.2	7.66	0.8	1.16	0.94	3.56	124	3.05	0.51												
73.2	142	58	13.5	0.14	13.8	2.13	3.1	1.23	7.69	1.07	252	9.33	7.43	9.12	0.96	0.67	0.3	8.08	81.4	3.23	0.52												
57.9	119	46.4	13.3	0.06	15.1	2.66	4.27	1.92	12.6	1.75	300	14.4	14.6	8.09	0.58	0.81	0.17	23.6	132	3.83	0.57												
57.6	132	51	14.6	0.06	16.8	2.99	4.42	1.98	12.6	1.72	332	14	13.8	10900	0.68	0.25	0.18	55.3	126	2.85	0.58												
65	126	51.1	14	0.07	15.8	2.72	4.35	1.98	12.6	1.78	367	15.4	15.1	8.1	0.61	0.43	0.34	17.6	150	4.14	0.68												